Solid State Communications, Vol. 68, No. 6, pp. 591–594, 1988.
Printed in Great Britain.

0038–1098/88 $3.00 + .00
Pergamon Press plc

INTERBAND CRITICAL POINT PARAMETERS DETERMINED BY ELLIPSOMETRY IN $Zn_xHg_{1-x}Se$

K. Kumazaki

Hokkaido Institute of Technology, Teine, Nishi-ku, Sapporo 006, Japan

and

L. Viña*, C. Umbach† and M. Cardona

Max-Planck-Institut für Festkörperforschung, Heisenbergstrasse 1, 7000 Stuttgart 80, FRG

(*Received* 16 *June* 1988 *by M. Cardona*)

The dielectric functions of $Zn_xHg_{1-x}Se$ crystals with $x = 0$ to 0.40, were measured by ellipsometry at room temperature between 1.8 and 5.5 eV. The E_1 and $E_1 + \Delta_1$ gaps showed a quadratic dependence on composition, while a linear one was obtained for the Δ_1 spin–orbit splitting. The broadening of the observed structures increases with x due to alloying effects. The results are discussed in comparison with those obtained for $Cd_xHg_{1-x}Te$.

1. INTRODUCTION

$Zn_xHg_{1-x}Se$ (ZnHgSe) CRYSTALS are a mixture of a semimetal HgSe and a wide-gap semiconductor ZnSe. They crystallize in the zincblende structure in the whole range of composition x. The value of the fundamental energy gap, E_0, of these crystals varies with x continuously from $E_0 = -0.02$ eV to $E_0 = 2.8$ eV [1].

Recently, phonon frequencies and plasmon–LO phonon coupling effects were measured in ZnHgSe from far infrared reflection spectra [2]. The optical properties at energies greater than those of E_0 are of interest because direct information about the band structure of the semiconductor alloys can be obtained from the Van-Hove singularities in the optical spectra. However, to our knowledge, there is no report on the optical properties and interband transitions, above the fundamental band gap, in ZnHgSe. The purpose of this paper is to determine accurately higher energy gaps in ZnHgSe crystals and to investigate the alloy-induced bowing and broadening effects.

2. EXPERIMENTAL PROCEDURES

ZnHgSe single crystals, with $x = 0$, 0.05, 0.10, 0.20, 0.30 and 0.40, were grown by a Bridgman method similar to that reported for HgSe [3] and CdHgSe [4]. As-grown samples were annealed in a Se-saturated atmosphere for one month. The composition of the samples was determined by an EPMA analysis. The electron concentration and Hall mobility were measured by the van der Pauw method.

The complex dielectric functions $\varepsilon(\omega) = \varepsilon_1(\omega) + i\varepsilon_2(\omega)$ were obtained at room temperature with an automatic rotating-analyzer ellipsometer discussed elsewhere [5]. The (1 0 0) surfaces to be measured were mechanically polished with Syton (Monsanto trade mark). The samples, mounted in a windowless cell in flowing dry N_2, were etched prior to measurement with bromine-methanol solutions and stripped with methanol and distilled water.

3. RESULTS AND DISCUSSION

The electron concentration and Hall mobility of the samples were 2–5 $\times$ 10^{17} cm^{-3} and about 1 $\times$ 10^4 cm^2 V^{-1} sec^{-1} at room temperature, respectively. The deviation of x was $\pm 5\%$ for $x = 0.05$ to 0.30 and $\pm 15\%$ for $x = 0.40$.

Figure 1 shows the real (ε_1) and imaginary (ε_2) part of the pseudodielectric function of ZnHgSe, at room temperature, for three selected compositions ($x = 0$, 0.05 and 0.30) as a function of photon energy. The values of ε_1 decrease rapidly from 9 to 2 as the photon energy increases from 2.5 to 3.5 eV. On the other hand, the ε_2 have a peak near 3 eV. The main peak in ε_2 corresponds to the E_1-singularity, while the $E_1 + \Delta_1$-gap is only seen as a shoulder at slightly larger energies. We observe a shift of the peak in ε_2 and

* Present address: Instituto de Ciencia de Materiales del Consejo Superior de Investigaciones Cientificas, Universidad de Zaragoza, E-50009 Zaragoza, Spain.
† Present address: Department of Applied Physics, 212 Clark Hall, Cornell University, Ithaca, New York 14853.

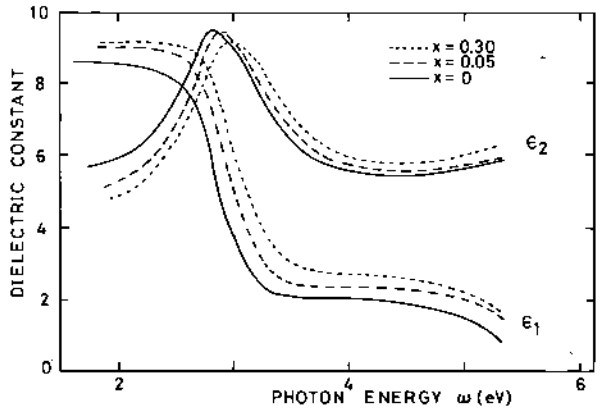

Fig. 1. Real (ε_1) and imaginary (ε_2) part of the pseudo dielectric function of ZnHgSe with $x = 0$, 0.05 and 0.30, at room temperature, as a function of photon energy.

the edge in ε_1 to higher energies with increasing x. A similar behavior was observed for the rest of the samples. In order to resolve the structure present in the spectra and obtain the critical point parameters we calculate numerically the second derivative spectra of the complex dielectric function from our ellipsometric data. The derivative spectra were fitted by assuming a two-dimensional saddle point for the E_1 and $E_1 + \Delta_1$ singularities.

The critical point energies and spin–orbit splitting are shown in Fig. 2 as a function of x. The value of the spin–orbit splitting Δ_1 was obtained by subtraction of E_1 from $E_1 + \Delta_1$. The E_1 structure corresponds to

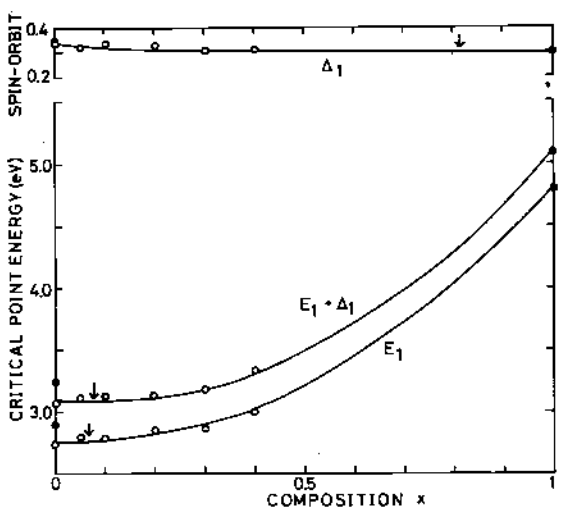

Fig. 2. Composition dependence of critical-point energies and spin-orbit splitting of ZnHgSe. Open circles are our data. The solid line represents the best fits of our data to a quadratic function. Arrows denote the minimum points.

Table 1. Values of the parameters a, b, c obtained by fitting the critical-point energy E vs composition x to the equation (1)

Critical point	Compound	a (eV)	b (eV)	c (eV)
E_1	ZnHgSe	2.781	−0.31	2.3
	CdHgTe	2.147	0.44	0.7
$E_1 + \Delta_1$	ZnHgSe	3.120	−0.41	2.4
	CdHgTe	2.778	0.47	0.6
Δ_1	ZnHgSe	0.339	−0.101	0.062
	CdHgTe	0.631	0.031	−0.079
E_2	ZnHgSe	–	–	–
	CdHgTe	4.468	0.66	−0.06

transitions from the $\Lambda_{4,5}$ valence band to the Λ_6 conduction band, while $E_1 + \Delta_1$ is associated to transitions from the Λ_6 valence band to the Λ_6 conduction band in an extended region of the Brillouin zone. Our data are depicted as open circles and the closed circles, for $x = 0$ and 1, taken from reflection measurements [6], are shown for comparison. The results show a quadratic dependence for the E_1 and $E_1 + \Delta_1$ gaps on composition, as in many other semiconducting mixed crystals [5–8], while an almost linear dependence is obtained for the Δ_1 splitting. The solid lines correspond to the best fit of our data, together with the values determined by the peak position of reflection for $x = 0$ [6] and by the lineshape analysis of reflection for $x = 1$ [6], to the following expression,

$$E(x) = a + bx + cx^2. \qquad (1)$$

The values of a, b and c for the two structures are listed in Table 1 together with those obtained from ellipsometric measurements for CdHgTe [5]. The magnitude and sign of the coefficient a for the E_1 and $E_1 + \Delta_1$ gaps are similar in both crystals, while those of the coefficients b and c are quite different. Namely, the coefficient b for ZnHgSe is negative and the value of c is about 3 or 4 times larger than that for CdHgTe. The trend for Δ_1 is similar for both systems.

The bowing in the quadratic dependence of the energy thresholds on composition can be separated in two contributions. One is an intrinsic bowing, present already in the virtual crystal approximation of alloys, as a consequence of the dependence of the lattice constant on x [5] and the second is an extrinsic bowing, the difference between intrinsic and experimental bowing, being due to effects of the random potential of the alloy. The difference in the lattice constant, $\Delta a/a$, for ZnHgSe, is 7%, while it amounts to only 0.3% for CdHgTe. Thus the larger bowing parameter, c, in ZnHgSe, is probably related to the

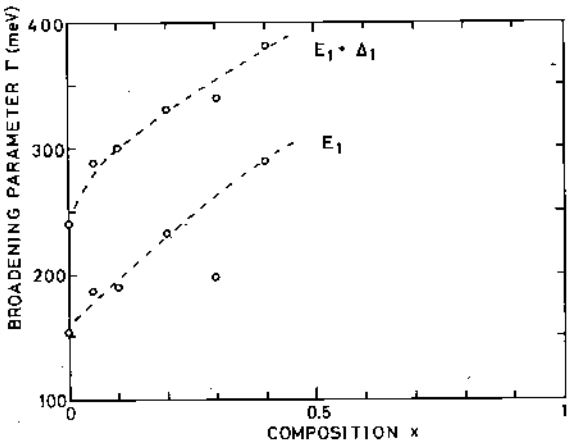

Fig. 3. Composition dependence of critical-point broadening parameters.

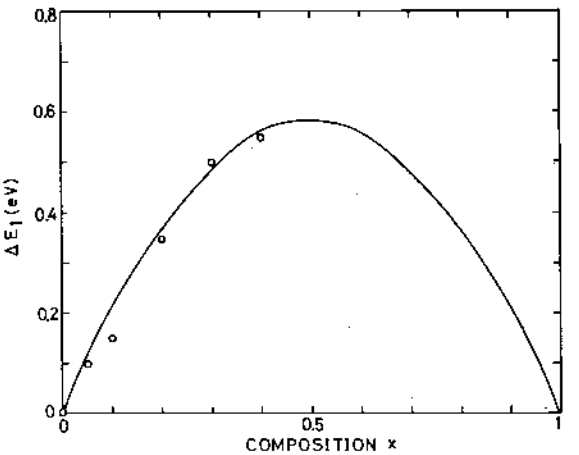

Fig. 4. Composition dependence of the difference between the experimental energy threshold values for the E_1 singularity and the values obtained by linear interpolation between HgSe and ZnSe. The solid line represents the parabolic relation $cx(1-x)$ with c obtained by fitting $E_1(x)$ to equation (1).

larger difference in the lattice constant [7]. The negative value of b implies the existence of a minimum (denoted by an arrow in Fig. 2) in the critical point energy at $x > 0$. This feature is also seen in other compounds [8]. We will not discuss the extrinsic bowing effect because there is no theoretical estimate of the bowing parameter for ZnHgSe [8].

The Lorentzian broadening parameters Γ [5], obtained assuming two-dimensional critical points for the E_1 and $E_1 + \Delta_1$ critical points, are shown in Fig. 3 as a function of x. The dashed lines are drawn through the experimental points only to visualize the dependence on composition. The broadening of the $E_1 + \Delta_1$ critical point is larger than that of the E_1 structure, and the values of Γ increase with increasing x. These features have also been reported for CdHgTe [5] and other ternary compounds [8]. However, our values of Γ for the $E_1 + \Delta_1$ and E_1 critical points in HgSe ($x = 0$) are larger, by a factor of 2 and 3 respectively, than those obtained in HgTe [5]. This large difference may be due to surface effects as seen in far infrared and Raman measurements in both compounds [9–14]. The surface conditions are different in both systems: it is difficult to obtain with our etchant as good surfaces in HgSe, CdHgSe and ZnHgSe as those obtained in HgTe and CdHgTe [5]. The optical constants of HgSe and HgTe differ considerably from each other, when we examine them in detail, especially in the far infrared spectra [9, 10] and in the Raman spectra [11–14]. We believe that one possibility for this is the difference in chemical activity of the surfaces. For example, the etching figures are very different [15]. We found marked difference in the dielectric functions for the (1 0 0) and (1 1 1) surfaces in HgSe [16]. We observed the deviation of x and the effect of inhomogeneity on plasmon-LO phonon coupling modes in FIR reflection measurements of ZnHgSe [2]. Recently a difference of Γ by a factor of 2 for E_1 was also observed in two different GaP [17]. Another possibility of the larger broadening observed here may be inhomogeneities in the composition.

We would like to point out that we could not see a possible maximum of Γ, observed near $x = 0.8$ in CdHgTe [5], because of the lack of samples with composition larger than 0.4.

In Fig. 4 we plot the difference ΔE_1 between the observed $E_1(x)$ gaps and the linear interpolation between the E_1 gaps of HgSe and ZnSe. The solid curve is calculated with the relation $cx(1-x)$, with c obtained by fitting $E_1(x)$ to equation (1). This curve shows a parabolic dependence symmetric with respect to $x = 0.5$. A similar behavior was found also for the $E_1 + \Delta_1$ gap. However, we cannot rule out the possibility of an asymmetric feature as observed in CdHgTe [5], since our present data do not extend beyond $x = 0.4$.

In conclusion, the critical point energies of the two structures E_1 and $E_1 + \Delta_1$ in ZnHgSe have been measured as a function of the composition by means of ellipsometry. These critical points have a positive bowing parameter c, while the dependence of Δ_1 on x is almost linear. The dependence of the critical point energies on composition of ZnHgSe is similar to that of CdHgTe. The large broadening parameters for ZnHgSe may stem from larger surface effects compared to those for CdHgTe.

Acknowledgements — One of the authors (K.K.) thanks the Max–Planck–Gesellschaft for the support

during his stay. He is also grateful to the HIT special Foundation, the Suhara Memorial Foundation and the Private College Promotion Foundation for their financial support.

REFERENCES

1. N.P. Gaveleshko, W. Dobrowolski, M. Baj, L. Dmowski, T. Dietl & V.V. Khomyak, Proc. 3rd Int. Conf. Physics of Narrow-Gap Semiconductors, Warsaw 1977, p. 331 (Edited by Raaluskiewicz, M. Gorska & E. Kaczmarek), PWN-Polish Scientific Pub., Warsaw and North Holland, Amsterdam (1978).
2. K. Kumazaki & N. Nishiguchi, *Solid State Commun.* **60,** 301 (1986).
3. K. Kumazaki, E. Matsushima & A. Odajima, *Phys. Status Solidi (a)* **37,** 579 (1976).
4. K. Kumazaki, N. Nishiguchi & M. Cardona, *Solid State Commun.* **58,** 525 (1986).
5. L. Viña, C. Umbach, M. Cardona & L. Vodopyanov, *Phys. Rev.* **B29,** 6752 (1984).
6. Landolt–Börnstein, vol. 17b, p. 478 and 390 (Edited by O. Madelung, M. Schult & H. Weiss), Springer, Berlin, Heidelberg, New York (1982).
7. A. Zunger & J.E. Jaffe, *Phys. Rev. Lett.* **51,** 662 (1983); K.C. Haas, H. Ehrenreich & B. Velicky, *Phys. Rev.* **B27,** 1088 (1983).
8. M. Cardona, *Phys. Rev.* **129,** 69 (1963).
9. A. Manabe, H. Noguchi & A. Mitsuishi, *Phys. Status Solidi (b)* **90,** 157 (1978).
10. A.M. Witowski & M. Grynberg, *Phys. Status Solidi (b)* **100,** 389 (1980).
11. P.M. Amirtharaj, K.K. Tiong & F.H. Pollak, *J. Vac. Sci. Technol.* **A1,** 1744 (19983).
12. K.K. Tiong, P.M. Amirtharaj, P. Parayanthal & F.H. Pollak, *Solid State Commun.* **50,** 891 (1984).
13. K. Kumazaki & M. Cardona, Proc. 9th Int. Conf. Raman Spectroscopy, Tokyo 1984, p. 662 (Edited by M. Tsuboi), The Chem. Soc. Japan, Tokyo (1984).
14. K. Kumazaki, to be published.
15. For example, E.P. Warekois, M.C. Lavine, A.N. Mariano & H.C. Gatos, *J. Appl. Phys.* **33,** 690 (1962).
16. Unpublished data.
17. S. Zalher, to be published.